

# Suppression of Nonradiative Recombination by V-Shaped Pits in GaInN/GaN Quantum Wells Produces a Large Increase in the Light Emission Efficiency

A. Hangleiter,<sup>1,\*</sup> F. Hitzel,<sup>1,†</sup> C. Netzel,<sup>1</sup> D. Fuhrmann,<sup>1</sup> U. Rossow,<sup>1</sup> G. Ade,<sup>2</sup> and P. Hinze<sup>2</sup>

<sup>1</sup>*Institute of Applied Physics, Technical University of Braunschweig, Mendelssohnstr. 2, D-38106 Braunschweig, Germany*

<sup>2</sup>*Physikalisch-Technische Bundesanstalt, Bundesallee 100, D-38116 Braunschweig, Germany*

(Received 10 March 2005; published 14 September 2005)

Despite the high density of threading dislocations generally found in (AlGaIn)N heterostructures, the light emission efficiency of such structures is exceptionally high. It has become common to attribute the high efficiency to compositional fluctuations or even phase separation in the active GaInN quantum well region. The resulting localization of charge carriers is thought to keep them from recombining non-radiatively at the defects. Here, we show that random disorder is not the key but that under suitable growth conditions hexagonal V-shaped pits decorating the defects exhibit narrow sidewall quantum wells with an effective band gap significantly larger than that of the regular *c*-plane quantum wells. Thereby nature provides a unique, hitherto unrecognized mechanism generating a potential landscape which effectively screens the defects themselves by providing an energy barrier around every defect.

DOI: [10.1103/PhysRevLett.95.127402](https://doi.org/10.1103/PhysRevLett.95.127402)

PACS numbers: 78.67.De, 61.72.Ff, 73.50.Gr

Light emission from semiconductors and semiconductor heterostructures is subject to competition between radiative and nonradiative recombination of electron-hole pairs. Only for highly perfect crystalline material with a low number of “deep” defect states, the nonradiative recombination probability is low enough to allow for a significant fraction of the electron-hole pairs to recombine radiatively.

In fact, conventional semiconductor wisdom “knows” that significant numbers of structural imperfections and defects either prohibit light emission at all or make the structures degrade quickly. For instance, in AlGaInP-based red light emitting diodes (LED’s) a dislocation density of more than  $10^3 \text{ cm}^{-2}$  reduces the radiative efficiency by more than an order of magnitude.

This was the background when in 1994 Nakamura *et al.* [1] reported their first blue LED exceeding 1 cd in brightness. The device was made from a GaInN/GaN heterostructure epitaxially grown on a highly dissimilar substrate, namely, sapphire. Because of the 30% difference in lattice constant, a large number (up to  $10^{10} \text{ cm}^{-2}$ ) of “threading dislocations” running along the (0001) growth direction plagues the material and intersects the active light emitting layers [2]. As for a “normal” semiconductor one would not expect any light emission at all at such high defect density; the high brightness even of these early devices was highly surprising. Later on, even higher efficiency was obtained using quantum well active regions [3,4].

As the active GaInN layers exhibited optical properties highly unusual for III-V semiconductors [5,6], it was suggested that excitons localized at compositional fluctuations or even quantum dots play a dominant role [7,8]. This kind of random localization of excitons was proposed to prohibit nonradiative recombination of the excitons at threading dislocations [7]. It appeared to be supported by transmission electron microscope (TEM) images showing small dotlike structures [9]. On the other hand, recent

detailed TEM studies indicate that such dotlike structures may be artifacts due to radiation damage during TEM observation [10].

As far as the optical properties were concerned, however, it was soon recognized that due to the lattice mismatch between GaInN and GaN (or between GaN and AlGaIn) and the resulting pseudomorphic strain field, the highly polar lattice leads to a strong piezoelectric polarization [11] inside the quantum wells. The huge internal field [of the order MV/cm [12]] in turn gives rise to a strong “quantum confined Stark effect” (QCSE) first observed in GaAs-based quantum wells [13]. In addition to a strong redshift of the emission [14], a dramatic reduction of the oscillator strength may thus result from these fields [15,16]. In fact, most of the unusual optical properties of nitride quantum wells may be well understood on the basis of the polarization fields [17]. However, the internal fields alone provide no explanation of the unusually large emission efficiency of such structures, even though they may enhance the effect of fluctuations [18]. On the contrary, one might expect an even smaller efficiency due to the reduced oscillator strength.

Epitaxial growth of group-III nitrides by means of metal-organic vapor-phase epitaxy (MOVPE) typically requires growth temperature in excess of  $1000^\circ\text{C}$  [19], due to the large binding energies of the species involved. At lower temperature and at low V-III ratio, the epitaxial layers tend to grow in a faceted manner. In other words, in order to achieve smooth planar surfaces, high temperature and large V-III ratio are required.

However, if In is to be incorporated into the layers, the low binding energy of InN and the large vapor pressure of N forces the use of much lower temperatures, typically around  $800^\circ\text{C}$ . At such low temperatures, even small perturbations of the surface tend to grow into (inclined) facets with the lowest growth rate, i.e., (1101) facets. This

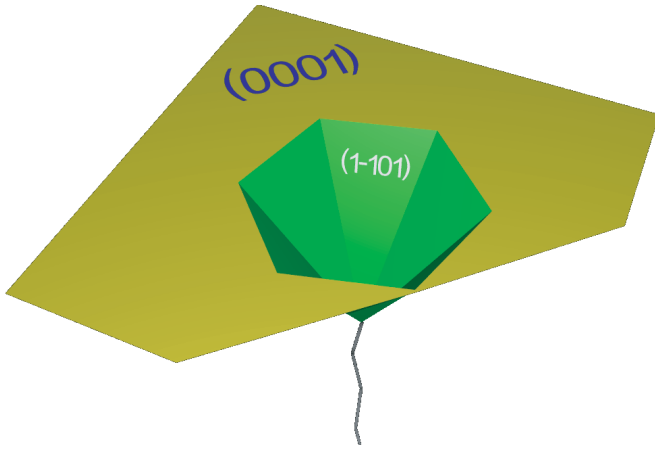


FIG. 1 (color). Schematic view of a hexagonal V-shaped pit emerging at the apex of a threading dislocation in a GaInN-based heterostructure.

is particularly true at the apex of threading dislocations, where V-shaped hexagonal pits with  $(1\bar{1}01)$  sidewalls appear [20,21] (c.f. Fig. 1). Using atomic force microscopy (AFM), one realizes that under suitable conditions virtually every threading dislocation is decorated with such a pit.

If thick layers of GaInN are grown, the pits become very large and finally cover the whole surface. In incorporation in the faceted area increases and a strongly inhomogeneous composition results [22]. In case of thin GaInN quantum wells with thicknesses of 5 nm and less, growth remains regular and well-defined pits evolve for multiple quantum well structures [20,21].

We have grown a variety of both undoped GaInN/GaN quantum well structures and full LED structures using low-pressure metal-organic vapor-phase epitaxy (commercial AIX200RF reactor) on (0001) sapphire substrates [23]. After a thin low-temperature GaInN nucleation layer and a 2  $\mu\text{m}$  thick GaN buffer layer, single or multiple

GaInN/GaN quantum wells were grown at 835 °C (total pressure 200 mbar, total flux 4.5 slpm, ammonia flow 2000 sccm, precursors triethylgallium and trimethylindium, carrier gas  $\text{N}_2$ ), capped by a 10 nm AlGaIn electron barrier and a 150 nm GaN capping layer. These structures were characterized by temperature and excitation power dependent photoluminescence (PL) measurements as well as on-wafer P(I) measurements in case of LED structures. Optimization of the growth procedure led to measured internal efficiencies of up to 73% and on-wafer external efficiencies of LED's up to 4.6%, both at room temperature (RT) [23]. Cross-sectional transmission electron microscopy (TEM) was carried out in a Philips CM 200 FEG microscope operated at 200 kV.

Systematic studies of the temperature and power dependent PL led us to the conclusion that random localization is only a minor effect at RT and that carriers are mainly present in form of mobile free excitons [23]. Spectroscopic scanning near-field optical microscopy on our samples revealed that small areas close to threading dislocations exhibit an emission about 300–400 meV higher in energy than the main photoluminescence peak. This led us to the conclusion that a higher band gap around every defect might form an energy barrier, which keeps carriers from reaching the defects and from recombining nonradiatively [24].

Cross-sectional transmission electron microscopy of optimized quantum well (QW) structures shows that highly perfect interfaces are obtained for *c*-plane QW's. A TEM image of a typical multiple quantum well (MQW) structure of this kind is shown in Fig. 2. In this case, the QW's have a thickness of 3.5 nm and a period of 11 nm on the (0001) plane. However, in the vicinity of a threading dislocation the QW's clearly follow a V-shaped pit. Inside the pit, the quantum wells grown on the  $(1\bar{1}01)$  sidewalls exhibit a much smaller thickness. Moreover, the barrier between the QW's on the sidewalls of the pit is also much thinner than

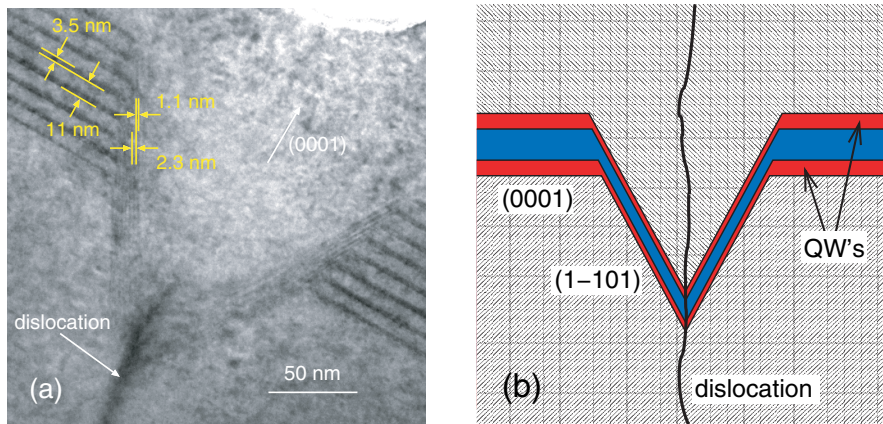


FIG. 2 (color). Transmission electron microscope image (a) of a GaInN/GaN multiple quantum well structure. In the planar region high quality QW's with well-defined sharp interfaces are visible. In the vicinity of a threading dislocation, a V-shaped pit appears with sidewall QW's with a thickness and spacing much lower than for the (0001) QW's. This is also schematically shown in (b).

in case of the  $c$ -plane QW's. This is also shown schematically in Fig. 2(b).

For this structure we find a QW spacing of 2.3 nm on the ( $\bar{1}\bar{1}01$ ) sidewalls, compared to 11 nm on the (0001) plane. The QW width is determined to approximately 1.1 nm on the sidewalls of the pit compared to 3.5 nm on the (0001) plane. On the other hand, considering that the growth of the barriers and of the QW's is under identical conditions except for the In incorporation, we expect the QW thickness to scale the same way as the QW spacing. Consequently, for the 3.5 nm  $c$ -plane QW in Fig. 2 the associated thickness of the sidewall QW's would be only about 0.7 nm, somewhat less than the 1.1 nm determined directly. Given the uncertainties in both methods to determine the QW width together with fluctuations between different pits, we use  $0.9 \pm 0.3$  nm as the reduced QW width.

It is interesting to note that in a simple-minded geometric view one would expect the growth rate on the facets to scale as the cosine of the angle, giving a ratio of 0.47 between the ( $\bar{1}\bar{1}01$ ) and the (0001) planes. The experimental value is around 0.25 showing that growth on the ( $\bar{1}\bar{1}01$ ) facet is much slower than on the  $c$  plane under the conditions used. This explains why pits develop at all and tend to get larger with increasing layer thickness.

Now, if the sidewall QW's are that much thinner than the  $c$ -plane QW's, quantum confinement together with a reduced QCSE would lead to a considerably larger band gap of the sidewall QW's. In Fig. 3 we compare the reduction of thickness obtained from the present TEM data to the change in emission energy obtained from spectroscopic scanning near-field microscopy (SNOM) [24]. Figure 3(a) shows low-temperature emission spectra obtained from different nm-sized areas of a (different) sample with two 2.5 nm GaInN QW's. While spectra obtained between defects (black) exhibit only the 430 nm main

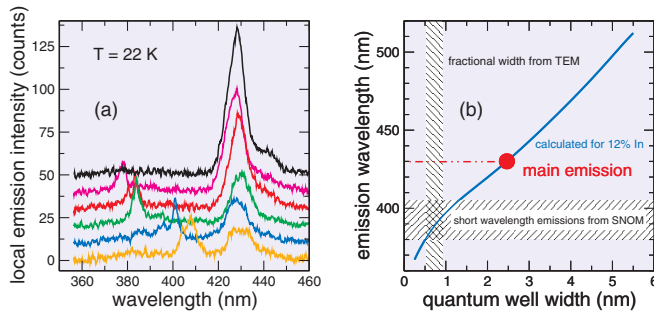


FIG. 3 (color). Comparison of TEM and near-field PL data: (a) shows low-temperature emission spectra obtained from nm-sized areas close to threading dislocations with a near-field microscope [24]. Besides the main emission at 430 nm multiple sharp peaks from different locations appear in the range 380–410 nm. Utilizing the calculated emission wavelength vs QW width we compare the  $c$ -plane QW and the sidewall QW widths (reduction ratio from Fig. 2) with the main emission and the short wavelength emissions observed in SNOM measurements.

QW emission, spectra from areas close to defects show additional emission peaks in the 380–410 nm range.

In order to compare the SNOM data with the TEM results, we use the calculated dependence of emission wavelength on well thickness, as shown in Fig. 3(b). The calculation is based on solving Schrödinger's equation for a quantum well with a built-in field, and utilizes the experimentally obtained band gap of GaInN [25] as well as the polarization field [12] as a function of In content. In addition, the field on the ( $\bar{1}\bar{1}01$ ) plane should be lower than on the (0001) plane for symmetry reasons, but this will have only a minor effect for such thin quantum wells. Clearly, the reduced QW thickness in the sidewall QW leads to an emission wavelength well within the range observed for the high-energy emission in the near-field measurements. In fact, from experiments with QW's grown on faceted laterally overgrown GaN/SiC structures we know that inclined QW's on ( $\bar{1}\bar{1}01$ ) facets do exhibit much shorter wavelength emission [26].

The presence of V-shaped pits and of thin sidewall QW's is clearly associated with high internal efficiency. In fact, the TEM images together with atomic force microscope (AFM) images of uncapped samples suggest that practically every defect is decorated with such a pit. Moreover, we observe a reduced thickness of the sidewall QW's not only for rather thick QW's (as in Fig. 2, where the effect is seen most clearly in the TEM image) but also for QW's with thicknesses below 2 nm, which exhibit the highest internal efficiencies. On the other hand, nonoptimized samples exhibiting fairly low room temperature efficiency but good low-temperature PL reveal no evidence for such pits and sidewall QW's.

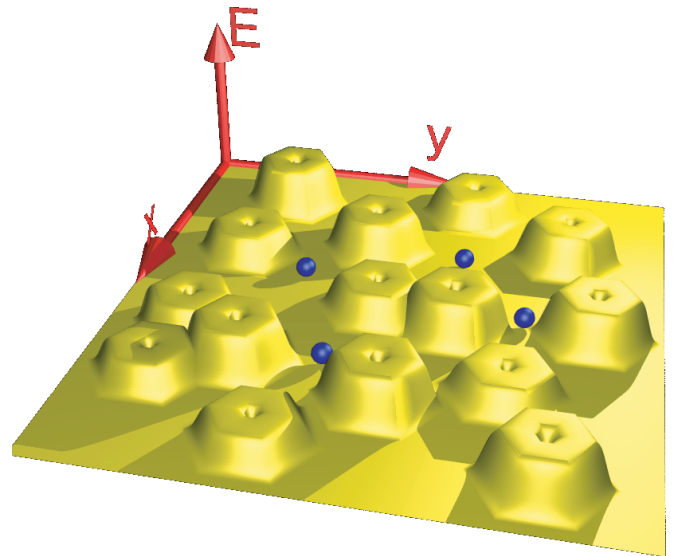


FIG. 4 (color). Visualization of the energy landscape resulting from V-shaped hexagonal pits exhibiting increased band gap in the sidewalls. Carriers in the regular  $c$ -plane QW's (with lower band gap) in between have to overcome a large energy barrier to reach the defects and to recombine nonradiatively.



Based on these observations we propose that suppression of nonradiative recombination in high efficiency GaInN/GaN quantum wells is due to a self-screening of the defects. The formation of V-shaped pits leads to narrow sidewall quantum wells surrounding every defect, with an effective band gap several hundred meV higher than that of the normal *c*-plane QW's. Thus an energy landscape as visualized in Fig. 4 emerges, where carriers are "antilo-calized" rather than localized. A barrier height of the order 400 meV as obtained from the near-field data [24] is sufficient to suppress nonradiative recombination even at room temperature.

It is interesting to note that to our knowledge so far no V-shaped pits have been reported for nitride QW's grown by molecular beam epitaxy (MBE). This may explain the common observation that MBE-grown GaInN-based LED's exhibit considerably lower efficiency than comparable MOVPE-grown devices, as there would be no self-screening of the defects in the MBE case.

Optimization of QW's for high efficiency therefore involves generating barriers around every defect. By maximizing the height of the barriers (i.e., thickness of the sidewall QW's) nonradiative recombination can be minimized. Doing this, one should keep in mind that the total fractional area of the pits should be as small as possible to maximize the area of the *c*-plane QW's emitting light at the design wavelength. On the other hand, to maximize radiative recombination a large excitonic oscillator strength and a small QCSE (i.e., narrow wells) should be provided.

In conclusion, using a combination of growth optimization, transmission electron microscopy, and scanning near-field optical microscopy we have obtained unambiguous evidence that the unexpectedly high emission efficiency of GaInN-based quantum well light emitting diodes relies on self-screening of defects rather than random localization. Hexagonal V-shaped pits decorating every threading dislocation can be forced to exhibit sidewall quantum wells with reduced thickness and higher band gap thus leading to a potential barrier around every defect, which keeps carriers from recombining nonradiatively at the defect.

The authors gratefully acknowledge partial financial support of this work by the Deutsche Forschungsgemeinschaft (DFG). Critical reading of the manuscript by H. Hillmer is highly appreciated.

---

\*Electronic address: a.hangleiter@tu-bs.de

†Now with Danish Micro Engineering A/S Transformervej 12, DK-2730 Herlev, Denmark.

- [1] S. Nakamura, T. Mukai, and M. Senoh, Appl. Phys. Lett. **64**, 1687 (1994).
- [2] S.D. Lester, F.A. Ponce, M.G. Craford, and D.A. Steigerwald, Appl. Phys. Lett. **66**, 1249 (1995).
- [3] S. Nakamura, M. Senoh, N. Iwasa, and S.-I. Nagahama, Appl. Phys. Lett. **67**, 1868 (1995).
- [4] S. Nakamura, M. Senoh, N. Iwasa, S.-I. Nagahama, T. Yamada, and T. Mukai, Jpn. J. Appl. Phys. **34**, L1332 (1995).
- [5] S. Chichibu, T. Azuhata, T. Sota, and S. Nakamura, Appl. Phys. Lett. **69**, 4188 (1996).
- [6] Y. Narukawa, Y. Kawakami, S. Fujita, S. Fujita, and S. Nakamura, Phys. Rev. B **55**, R1938 (1997).
- [7] S. Nakamura, Science **281**, 956 (1998).
- [8] K.P. O'Donnell, J.F.W. Mosselmanns, R.W. Martin, S. Pereira, and M.E. White, J. Phys. Condens. Matter **13**, 6977 (2001).
- [9] Y. Narukawa, Y. Kawakami, M. Funato, S. Fujita, S. Fujita, and S. Nakamura, Appl. Phys. Lett. **70**, 981 (1997).
- [10] T.M. Smeeton, M.J. Kappers, J.S. Barnard, M.E. Vickers, and C.J. Humphreys, Appl. Phys. Lett. **84**, 4110 (2004).
- [11] F. Bernardini, V. Fiorentini, and D. Vanderbilt, Phys. Rev. B **56**, R10024 (1997).
- [12] A. Hangleiter, F. Hitzel, S. Lahmann, and U. Rossow, Appl. Phys. Lett. **83**, 1169 (2003).
- [13] E.E. Mendez, G. Bastard, L.L. Chang, L. Esaki, H. Morkoc, and R. Fischer, Phys. Rev. B **26**, R7101 (1982).
- [14] T. Takeuchi, S. Sota, M. Katsuragawa, M. Komori, H. Takeuchi, H. Amano, and I. Akasaki, Jpn. J. Appl. Phys. **36**, L382 (1997).
- [15] J.S. Im, H. Kollmer, J. Off, A. Sohmer, F. Scholz, and A. Hangleiter, Phys. Rev. B **57**, R9435 (1998).
- [16] A. Hangleiter, J.S. Im, H. Kollmer, S. Heppel, J. Off, and F. Scholz, MRS Internet J. Nitride Semicond. Res. **3**, 15 (1998).
- [17] A. Hangleiter, in *Low-Dimensional Nitride Semiconductors*, edited by B. Gil (Oxford University Press, New York, 2002), Chap. 13.
- [18] M. Gallart, P. Lefebvre, A. Morel, T. Taliercio, B. Gil, J. Allegre, H. Mathieu, B. Damilano, N. Grandjean, and J. Massies, Phys. Status Solidi A **183**, 61 (2001).
- [19] H. Amano, N. Sawaki, I. Akasaki, and Y. Toyoda, Appl. Phys. Lett. **48**, 353 (1986).
- [20] I.-H. Kim, H.-S. Park, Y.-J. Park, and T. Kim, Appl. Phys. Lett. **73**, 1634 (1998).
- [21] Y. Chen, T. Takeuchi, H. Amano, I. Akasaki, N. Yamada, Y. Kaneko, and S.Y. Wang, Appl. Phys. Lett. **72**, 710 (1998).
- [22] K. Hiramatsu, Y. Kawaguchi, M. Shimizu, N. Sawaki, T. Zheleva, R.F. Davis, H. Tsuda, W. Taki, N. Kuwano, and K. Oki, MRS Internet J. Nitride Semicond. Res. **2**, 6 (1997).
- [23] A. Hangleiter, D. Fuhrmann, M. Grewe, F. Hitzel, G. Klewer, S. Lahmann, C. Netzel, N. Riedel, and U. Rossow, Phys. Status Solidi A **201**, 2808 (2004).
- [24] F. Hitzel, G. Klewer, S. Lahmann, U. Rossow, and A. Hangleiter, Phys. Status Solidi C **1**, 2520 (2004).
- [25] J. Wu, W. Walukiewicz, K.M. Yu, J.W.A. III, E.E. Haller, H. Lu, and W.J. Schaff, Appl. Phys. Lett. **80**, 4741 (2002).
- [26] F. Hitzel, U. Ahrend, N. Riedel, U. Rossow, and A. Hangleiter, Phys. Status Solidi C **0**, 2674 (2003).